

New approach to monitor bridge piers subjected to scour using rocking vibrations

M. Belmokhtar¹, F. Schmidt¹, A. Ture Savadkoohi², and C. Chevalier³

¹Univ Gustave Eiffel, MAST-EMGCU, Boulevard Newton, F-77454 Marne-la-Vallée, France

²Univ Lyon, ENTPE, LTDS UMR CNRS 5513, Rue Maurice Audin, F-69518 Vaulx-en-Velin, France

³Univ Gustave Eiffel, GERS-SRO, Boulevard Newton, F-77454 Marne-la-Vallée, France

Abstract

This work focuses on the dynamic behavior of bridge piers subjected to scour. Here, the paper is divided on two parts. The first part considers the model of bridge pier by assuming a rocking solid partially embedded in a Winkler soil with translational and rotational conditions at its base. Simple geometry and boundary conditions of bridge pier are represented because the aim of this work is to show the feasibility of a new method based on free response analysis for bridge piers subjected to scour in general case. In fact, this physical model coupling solid mechanics for the structure and the continuum mechanics for the soil makes it possible for us to identify experimentally two rocking modes. In that way, the second part shows an experimental campaign in laboratory implemented on reduced pier models embedded in Fontainebleau sand with different geometries and inertias. From frequency decomposition of signals, natural frequencies and shape modes highlighted by the model are identified and compared from experiments. Analytical formulations and experiments show the interest to use vibration-based monitoring for scouring.

1 Introduction

Detection and diagnosis of damages and faults in structural systems are important issues for punctual repairing and/or replacements of elements leading to prevention of losses including human, environmental and economy. Structural health monitoring techniques [1] are divided to several categories which we name here two major ones: i) Vibration based methods [2] which investigate on the changes of system properties in linear and/or nonlinear domains, such as frequencies, damping, linear or nonlinear normal modes, frequency responses and backbone curves [3, 4, 5, 6]; ii) Ultrasonic techniques which are mainly used for detection of small sized faults or early developments of damages via inspection of received simulated waves, generated by some transducers, for mapping variations of mechanical material properties [7, 8]. Monitoring the health state of bridges is of highly important due to their important roles in transportation and other communication means. One of main factors causing damages in bridges is scour [9, 10] which is removal of sediment and particles from around the bridge bases or piers. This phenomenon can danger the stability of the bridge and even causes its total collapse. A study of more than 500 bridge failures in US shows that more than 53 % of bridge failures are due to hydraulic risks leading to very expensive structural maintenance [11]. There are several costly technologies which are used for monitoring some parameters that are linked to the scour risk, e.g. water depth-measuring devices [12], magnetic sliding collars [13], float-out systems [14], radar systems [15] and time-domain reflectometry [16]. Considering the scour as a damage in a system leads to exploitation of vibration based damage detection techniques for its monitoring [17, 18, 19]. Several methods have been developed to detect changes of modal characteristics of the system, such as natural frequencies, mode shapes and dynamic rigidities [20, 21, 22, 23]. Numerical and experimental studies via auto-regressive moving average vector (ARMAV) [24, 25] show that modal characteristics of bridges change due to scour: an increase of scour depth leads to decrease of eigenfrequencies. Foti and Sabia [26] reported two distinct behaviors accompanied by scour: the elastic dynamic behavior of the bridge pier which can be represented by an assembly of Euler- Bernoulli beam models [27] and the rocking response observed mainly for massive bridge piers. To cope with these two phenomena, analytical and numerical models of bridge piers have been carried out. For dealing with the scour, water is often considered as an added mass to the overall system [28]. A bridge pier can be modeled as a partially embedded beam in soil, while experimental investigations show that the trend of the variation of the first natural frequency is close to that of a cantilevered beam model [29]. Boujia et al. [30, 31] performed analytical static studies leading to the definition of a fixed distance between the free length of a partially embedded beam in soil and an equivalent cantilevered beam. Belmokhtar et al. [32] provide a first order dynamical equivalence between a scoured beam and its equivalent cantilevered beam. Their developed works depend on the chosen soil-structure interaction model, linking the depth of the foundations, the geometry, the inertia of the structure and

the mechanical proprieties of the soil. Modeling the bridge pier as a cantilevered beam loses its accuracy where rocking behavior appears. Rocking modes are always observable. In modal analysis, these modes are named as the mode 0 which are solutions of an eigenvalue problem [33]. For massive bridge piers with shallow foundations, Bao et al. [34, 35] observed a predominance of the rocking mode at lower frequencies while the post processed data detects only this mode as the one affected by the scour. Boujia et al. [36] developed a model for rocking behaviors of the pier accompanied by experiments on a reduced model of a bridge piers in a water flume showing good agreements between predicted frequencies by the developed model, experimental results and those which obtained from finite element modeling of the system.

An important issue in modeling soil-structure interactions as a parameter of scour monitoring is to define the soil reaction. Studies which focus on the evolution of natural frequencies of the system, aim at represent the soil-structure interactions as elastic reactions: The most common method is to define the interactions with the Winkler model [37]. However, Winkler springs are originally defined for static cases while dynamical Winkler stiffness can be introduced, especially for rocking behaviors [29, 30, 35, 32]. Gazetas [38, 39] established a list of dynamic stiffnesses and dynamical impedances issued from Winkler modes [40]. Such developed techniques are applied for different systems and mechanical properties of the soil [41, 42, 43] for detection of variations of the stiffness as a function of embedded part, cross-section (circular or square) and the frequency: in many cases, hypothesis of the static stiffness derived from Winkler theorem is not enough. The focus of this paper is studying of the rocking vibration modes of bridge piers due to the scour via taking into account the dynamic Winkler soil model. The paper is organized as it follows: The dynamical mode of the partially embedded bridge pier and further analytical investigations are reported in Sect. 2. Some experimental works accompanied by a developed technique of post processing of data are reported in Sect. 3. Detection of rocking modes of the system and further discussion are presented in Sect. 4. Finally the paper is concluded in Sect. 5.

2 Dynamical modeling of rocking behavior under scour

In this Section, rocking vibration behavior of a pier partially embedded in an elastic soil is modeled.

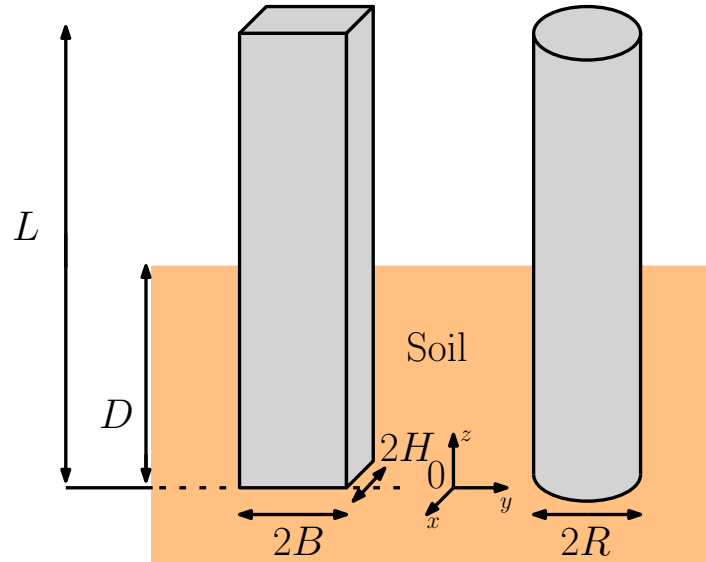


Figure 1: Geometric properties of rocking vibration behavior.

2.1 Framework

We would like to model bridge piers by the Euler-Bernoulli beam element. Let us consider two beams with different cross-sections which are depicted in Figure 1. In detail, one of them has a circular cross-section with the diameter of $2R$, while the cross-section of the second beam is rectangular with dimensions of $2B$ and $2H$. These beams are partially embedded in a soil which is supposed to be elastic. Due to the partially embedded part of the beam in the soil, it can present a transnational movement characterized by $u(z, t)$ standing for rigid mode of the beam, supplemented by a rotation named as $\theta(t)$. This phenomena is illustrated schematically in Figure 2: u_g and u_b are respectively displacements of the center of the gravity and the base while $\theta(t)$ is the rotation angle around a point. We use $\theta(t)$ and u_g variables to characterize a two degrees of freedom (dof) rocking behavior of the beam. In this work, we model the lateral soil reactions by the distributed Winkler springs k [41].

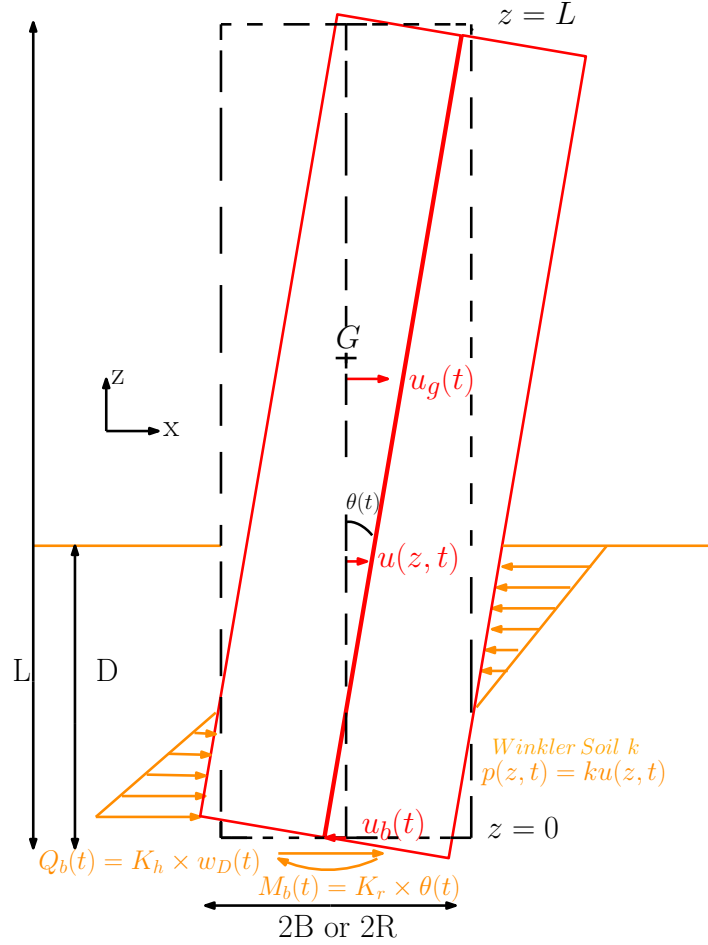


Figure 2: Model of a rocking pier of length L , width $2B$ and embedded length D .

We assume that $|\theta| \ll 1$ which leads to the linear rocking behavior of the pier. Then, the horizontal displacement along z -axis can be written as:

$$u(z, t) = \theta(t)z + u_b(t) = \theta(t) \left(z - \frac{L}{2} \right) + u_g(t). \quad (1)$$

The dynamic equilibrium at the center of gravity leads to:

$$\begin{cases} m\ddot{u}_g(t) + \int_0^D ku(z, t)dz + K_h u_b(t) = 0, \\ J\ddot{\theta}(t) - \int_0^D ku(z, t) \left(z - \frac{L}{2} \right) dz - \frac{K_h L}{2} u_b(t) + K_r \theta(t) = 0, \end{cases} \quad (2)$$

where m and J are respectively the mass and the inertia momentum of the pier, while K_h and K_r stand for translational and rotational rigidities of springs at the base of the pier [39, 41]. These springs can also result from the types of foundations (pile, footing,...). For our study we will suppose it as resulting from the tension and compressive states of the model soil-structure interaction studied in Section 3. Equations 1 and 2 permit to derive the following relation:

$$M \begin{pmatrix} \ddot{u}_g(t) \\ \ddot{\theta}(t) \end{pmatrix} + K(D) \begin{pmatrix} u_g(t) \\ \theta(t) \end{pmatrix} = 0, \quad (3)$$

where the mass matrix of the 2 dof system is:

$$M = \begin{pmatrix} m & 0 \\ 0 & J \end{pmatrix} \quad (4)$$

and the stiffness matrix is:

$$K(D) = \begin{pmatrix} kD + K_h & \frac{kD}{2}(D-L) - \frac{K_h L}{2} \\ \frac{kD}{2}(D-L) - \frac{K_h L}{2} & \frac{kD}{2} \left(\frac{2}{3}D^2 - LD + \frac{L^2}{2} \right) - \frac{K_h L^2}{4} + K_r \end{pmatrix} \quad (5)$$

Via Eq. 5 the scour of the bridge pier can be monitored by analyzing changes in stiffness matrix $K(D)$ due to the variation of the embedded length D .

2.2 Soil-Structure Interaction parameters

Coefficients of springs for modeling soil-structure interactions depend on: i) the embedded length of the beam, i.e. D ; ii) the geometry and the cross-section (rectangular or circular) of the pier [38, 39, 40, 41]. For distributed springs k , some formula are provided which depend on the D/R or D/B ratios and the Young modulus of the soil E_s . Moreover, springs of the base of the pier, K_h and K_r , are linked to the mechanical properties of the soil and the cross-section of the pier [38, 39, 41]. In this respect, the springs introduced in equation 2 can be expressed for following two cases:

- Circular cross section:

$$\begin{cases} k &= k(D, R) \approx 1.75 \left(\frac{D}{R}\right)^{-0.13} E_s, \\ K_h &= K_r(R) = \frac{2GR}{2 - \nu_s}, \\ K_r &= K_h(R) = \frac{8GR^3}{3(1 - \nu_s)}, \end{cases} \quad (6)$$

- Rectangular cross section:

$$\begin{cases} k &= k(D, B) \approx 2.18 \left(\frac{D}{B}\right)^{-0.13} E_s, \\ K_h &= K_r(R_0) = \frac{2GR_0}{2 - \nu_s}, \\ K_r &= K_h(R_{0r}) = \frac{8GR_{0r}^3}{3(1 - \nu_s)}, \end{cases} \quad (7)$$

where (R_0, R_{0r}) are equivalent radius associated to springs (K, K_r) [38]:

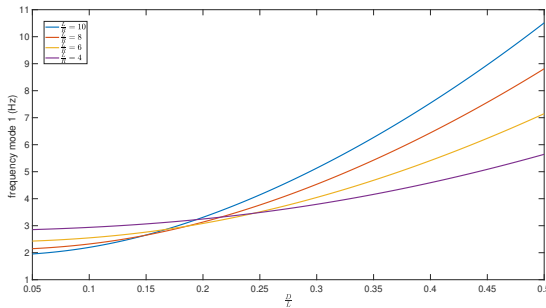
$$\begin{cases} R_0 &= \sqrt{\frac{2B \times 2H}{\pi}}, \\ R_{0r} &= \left(\frac{16HB^3}{3\pi}\right)^{1/4}. \end{cases} \quad (8)$$

2.3 Frequency domain analysis of scoured rocking behavior

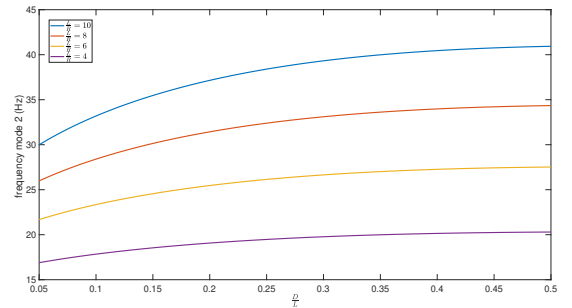
Eq. 3 in frequency domain reads following polynomial where its are the natural frequencies (ω_0) of the system:

$$P(\omega, D) = \det(K - \omega^2 M) = 0, \quad (9)$$

$P(\omega, D)$ is a fourth-degree polynomial of unknown ω . We assume that the system possesses only rocking modes and we admit only positive solutions of Let us suppose a circular pier with the length $L = 1 m$, Poisson ratio $\nu_s = 0.3$ and a mass density of $\rho = 2500 kg/m^3$. We set the Young modulus of soil $E_s = 2.5 MPa$. Figure 3 shows variations of two natural frequencies as function of the embedded length D/L obtained from solving Eq.(9). Figure 3a illustrates



(a) First natural frequency for different width as a function of the embedded length D/L .



(b) Second natural frequency for different width as a function of embedded length D/L .

Figure 3: Natural frequencies of circular pier with different slenderness ratio L/R .

the first natural frequency of the system described in Figure 2 for different values of the slenderness ratio L/R . It is seen that for higher values of L/R , the first natural frequency is more sensitive to the scour. While the second natural frequency of the system increases directly by increamenets of the ration of the slenderness, see Figure 3b.

3 Identification and vibration testing of rocking behavior

In this part, the method and the experimental setup for the study of a set of reduced models of bridge piers excited under impact are described. Different length, geometries and inertia are tested. On one hand, the signal processing method using modal analysis theory [33] will be detailed. On the other hand, a set-up for Experimental Modal Analysis (EMA) is carried out in order to identify modal parameters with a Frequency Domain Decomposition approach [44].

3.1 Modal parameters for rocking behavior identification

Modal Analysis is an effective method for describing, understanding and modeling the dynamic behavior of a structure. The concept of modal base (ϕ_r, ω_r^2) of the r -th mode makes it possible to decompose the energy information in each mode. Therefore, Equation 3 can be written as an eigenvalue problem:

$$(M^{-1}K)(D)\phi_r(D) = \omega_r(D)^2\phi_r(D), \quad (10)$$

where ω_r is the eigenfrequency or natural frequency of the r -th mode and the associated shape mode is:

$$\phi_r(D) = \begin{pmatrix} U_{gr}(D) \\ \Theta_r(D) \end{pmatrix}. \quad (11)$$

The components of ϕ_r do not have the same units, so physical representation and normalization does not make sense. Therefore, transformation of this vector is necessary, especially for measurements using accelerations. We made the choice to introduce a new shape mode ϕ'_r , defined as:

$$\phi'_r(D) = \begin{pmatrix} U_{1r}(D) = U_{gr}(D) - \Theta_r(D)\frac{L}{2} \\ U_{2r}(D) = U_{gr}(D) + \Theta_r(D)\frac{L}{2} \end{pmatrix}. \quad (12)$$

Obviously, this transformed problem can be expressed as an eigenvalue problem associated to the same natural frequencies ω_r as Equation (10):

$$(M'^{-1}K')(D)\phi'_r(D) = \omega_r(D)^2\phi'_r(D), \quad (13)$$

where K' and M' are symmetric matrices. The new formulation of the dynamic equilibrium is:

$$M' \begin{pmatrix} \ddot{u}_1(t) \\ \ddot{u}_2(t) \end{pmatrix} + K'(D) \begin{pmatrix} u_1(t) \\ u_2(t) \end{pmatrix} = 0. \quad (14)$$

In other terms, a transformed 2 Degrees-of-freedom (DOF) problem is formulated for EMA. This new modal approach is defined by considering the displacement of the two extremities of the pier (Figure 2):

$$(u_1(t), u_2(t)) = (u(0, t), u(L, t)). \quad (15)$$

Modal decomposition is implemented by solving numerically the eigenvalue problem written in Equation (10) and using Equation (12). In Figure 4, a circular pier rocking behavior is simulated for a slenderness ratio $L/R = 8$. Figure 4a plots frequency sensitivity under scour for each mode. The sensitivity is inversed for each mode: a raise for mode 1 and a decrease for mode 2 when the soil level is increasing. We can suppose that for low level of soil this two modes are far in terms of natural frequencies but it seems close when this level increase. Figure 4b plots shape modes with normalized displacement vector, as introduced in Equation (15):

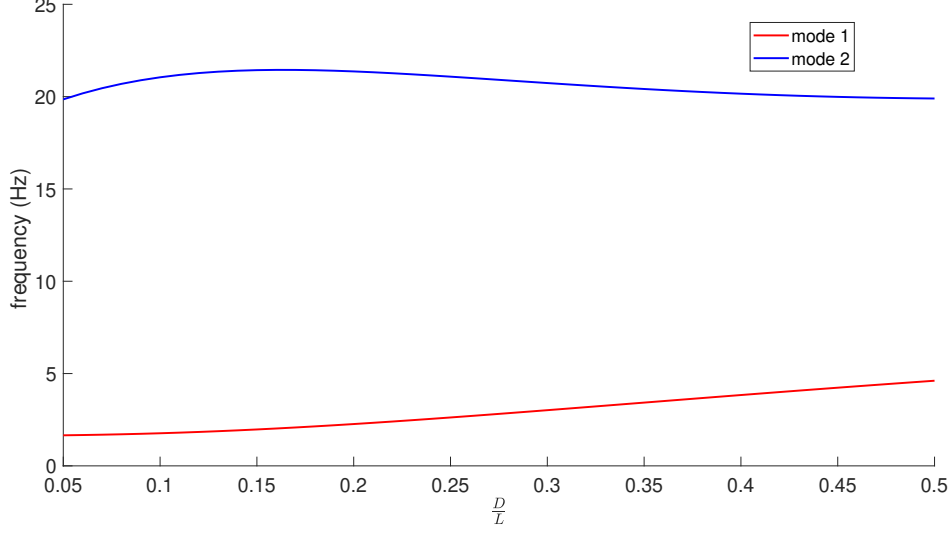
$$U_{2r}(D) - U_{1r}(D) = 1 \Leftrightarrow \Theta_r(D) = \frac{1}{L}. \quad (16)$$

In Figure 4b, the dashed line "-" is the embedded part of the shape mode. For each mode, we can observe a change of the center of rotation for different embedded length D . The shape of mode 1 is rotating around its base $z = 0$, whereas the shape of mode 2 is rotating around a point higher along the z -axis. With Figure 4 we conclude two different behaviors clearly identifiable when the soil level is low. It must be from the second mode which is including a higher translation at its base than the first mode but this difference become less when the soil block this translation i.e when the soil level is high.

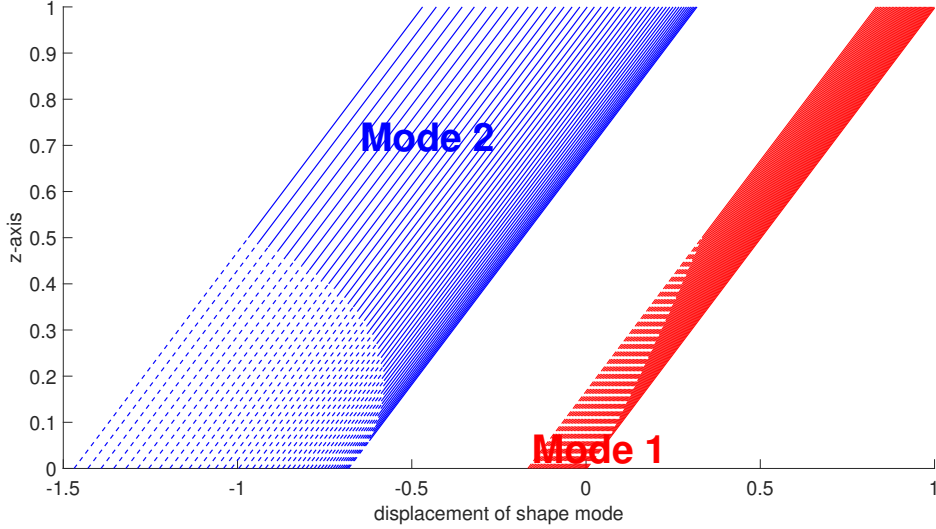
In the study, we focus on a new parameter for scoured bridge pier monitoring: the "center of rotation of the mode" of the mode r $z_{cr}(D)$ which is the center of rotation of the shape mode r : It is defined as the point where the displacement of the shape mode $U_r(z_{cr})$ is equal to 0. The center of rotation is non-dependent of the normalization of the shape mode $\phi_r(D)$ or $\phi'_r(D)$. In fact, with Equation (11) we can write:

$$z_{cr}(D) = \frac{L}{2} - \frac{U_{gr}(D)}{\theta_r(D)} = L \frac{U_{1r}(D)}{U_{1r}(D) - U_{2r}(D)}. \quad (17)$$

In Figure 5, the rotation center of each mode is plotted. Sensitivity of the shape mode to scour is clear on Figure 4b, with a higher value of rotation center of the mode 1 and a lower value for the mode 2.



(a) Natural frequencies $f_r(D/L) = \omega_r(D/L)/2\pi$ for $r \in [1, 2]$



(b) Shape modes with the following normalization $U_{2r}(D/L) - U_{1r}(D/L) = 1$

Figure 4: $(\omega_1(D/L), \omega_2(D/L))$ and $(\phi'_1(D/L), \phi'_2(D/L))$ for a circular pier with a slenderness ratio $R = L/8$

3.2 Experimental set-up

In order to identify modal parameters experimentally, extraction of poles of the transfer function is the most common method. The easiest way to obtain the transfer function is to excite all modes of the structure through an impact. As shown on Figure 6, for experiments, we built a pendulum system for the impact. In Figure 6a the same initial displacement ($\alpha = \text{constant}$) is given to ensure a repeatability of the test. Indeed, with constant α , the iron ball applies the same excitation on the structure (Figure 6b). The transfer function is directly approximated from output data collected by accelerometers. In total, three reduced-scale bridge piers are built, and their modal behavior tested in lateral direction x . In Table 1, the various bridge piers are presented, the bigger dimension of the rectangular structure is supported by y -axis. A is the area of the cross section. L is the length of the pier (two values are chosen: $0.75m$ with 4 positions of sensors and $1m$ with 5 positions of sensors). The instrumented piers are partially embedded by a length D and rests on a 10 cm soil bed. Then, the experimental protocol consists in the study of the response of the from D_{max} (25 cm for the pier 1 and 3 and 30 cm for pier 2) to D_{min} (10 cm for pier 1 and 5 cm for the pier 2 and 3) in steps of 5 cm. Also, each sensor records the acceleration for both x and y axis.

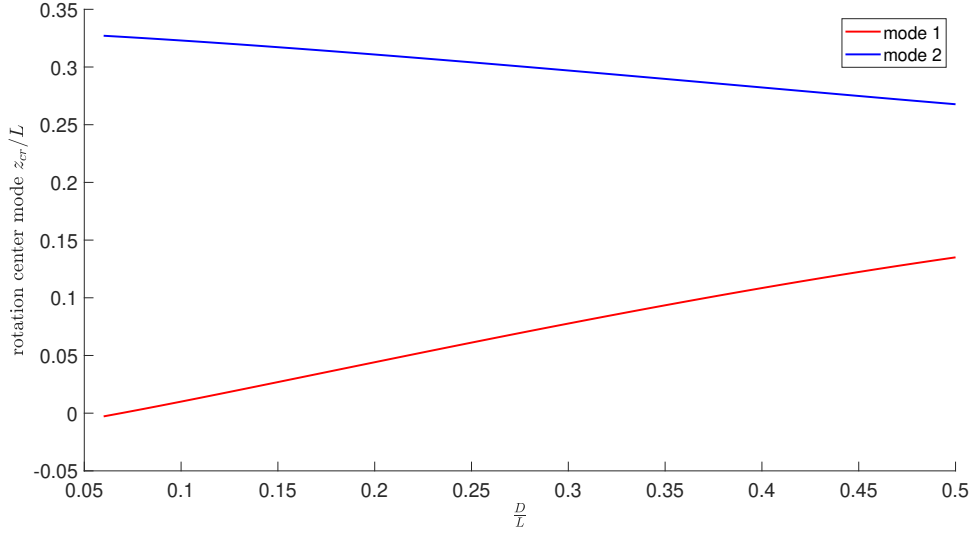


Figure 5: Center of rotation of the mode z_{cr}/L as a function of D/L .

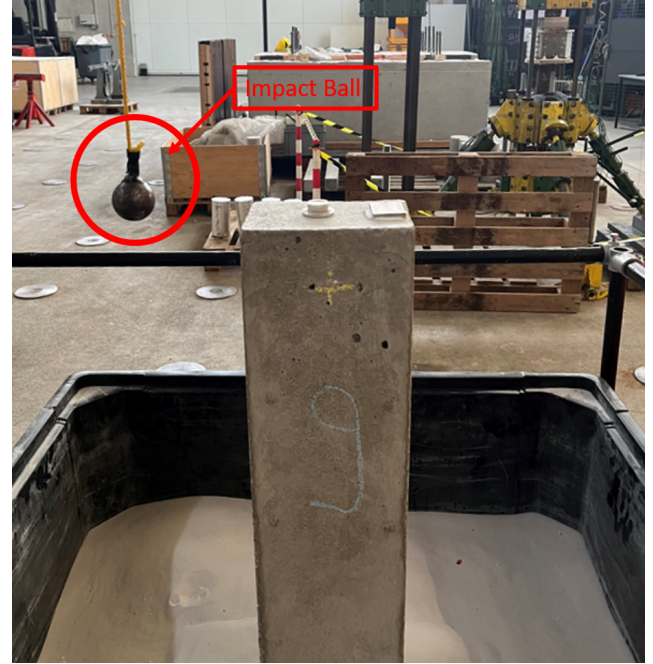
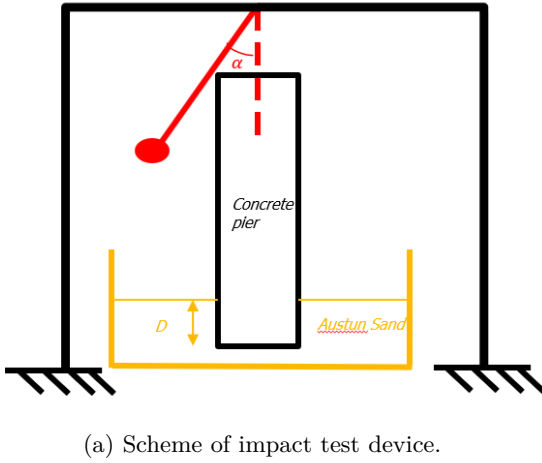


Figure 6: Experimental set up

3.3 Data processing

As explained in the previous section, the impact test excites many frequencies. For each pier, accelerometers collect data for the x and y axis. In Figure 7, the responses of pier n°2 under excitation for the x axis are plotted. Figure 7a shows the temporal response of each sensor in both directions. "Acc●x" corresponds on the accelerometer number ● in the x direction. Accelerometers are numeroted in the increasing order by strating from the top position of the pier to the bottom position. Figure 7b plots a zoom of the power spectral density (PSD) of each output plotted in Figure 7a. PSD is computed by analyzing the square of the modulus of the Fourier Transform of each signal. In Figure 7b, the two modes can be identified with the peak picking method, mainly due to the sensors in the same direction of the excitation. Concerning presented results in Figure 7, following remarks can be expressed: i) the second mode is highly damped compared to the first. ii) in Figure 7, the first mode along the y - axis (orthogonal to the excitation) can be

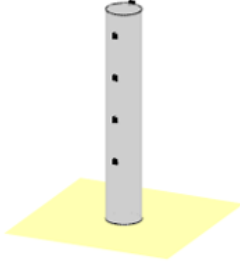
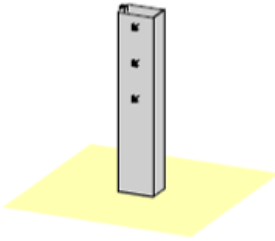
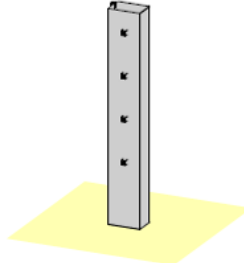
Pier n°	1	2	3
Type	circular	square	square
$L \times A \text{ (m}^3\text{)}$	$1.0 \times 0.16^2 \pi$	$0.75 \times 0.15 \times 0.10$	$1 \times 0.15 \times 0.10$
Position of sensors along z-axis (meter)	1-0.9-0.7-0.5-0.3	0.75-0.7-0.55-0.3	1-0.9-0.7-0.5-0.3
schema			

Table 1: Type of tested structures with position of sensors according to referential of Figure 2.

observed for sensors in this same direction: it is due to the less of precision on the targeted impact test.

Then, using several sensors allows us to use correlation between signals. Correlation between signals is a powerful mathematical tool for data processing as it reduces noise and modal parameters can be more easily identified. In fact, if we study the correlation between N output signals $y_{i \in [1, N]}$, we can introduce the temporal correlation matrix between signals: $(g_{yy}(\tau))_{ij}$ the correlation between signals $y_i(t)$ and $y_j(t)$ in the temporal space τ . By introducing the Hermitian matrix $(G_{yy}(p))_{ij}$ which is the Fourier transform of $(g_{yy}(\tau))_{ij}$, the singular value decomposition (SVD) gives the following relationship:

$$[G_{yy}(\omega)] = [U(\omega)] [S(\omega)] [V(\omega)]. \quad (18)$$

If we note N_s the number of sensors, $[G_{yy}(\omega)]$ is a $N_s \times N_s$ matrix which is named the power spectral density matrix. In figure 8, the first five singular values of $[G_{yy}]$ are plotted. Responses are uncorrelated to the noise and results are analyzed as a one degree of freedom system near the natural frequency. Near the mode k corresponding to the frequency ω_k , using Equation (18) [44, 19],

$$([U(\omega_k)])_1 \approx (\Phi)_k', \quad (19)$$

where $(\Phi)_k'$ is the shape vector of mode k . It is a vector column of $1 \times N_s$ size. According to Equations (18) and (19) and by assuming the hypothesis' of Section 3.1. Shape modes (FDD) are represented in Figure 4. For the representation, we made the choice to plot the modulus of the shape mode $((\Phi)_k')$ with the following normalization:

$$(\Phi)_k'^H (\Phi)_k' = 1, \quad (20)$$

where $(\Phi)_k'^H$ is the conjugate transpose of $(\Phi)_k'$. In Figure 9, a linear regression between each value of the vector $[U]$ is plotted. The two rocking modes are identified. We will discuss this aspect in more details in the following Section.

In Figure 9, for the second mode, linear regression has more residual errors than the mode 1. The shape modes are scaled according to the Table 1 with the euclidean norm of equation 20. One of the causes of this problem is, as already pointed out after analyzing Figure 7, the mode 2 is more damped.

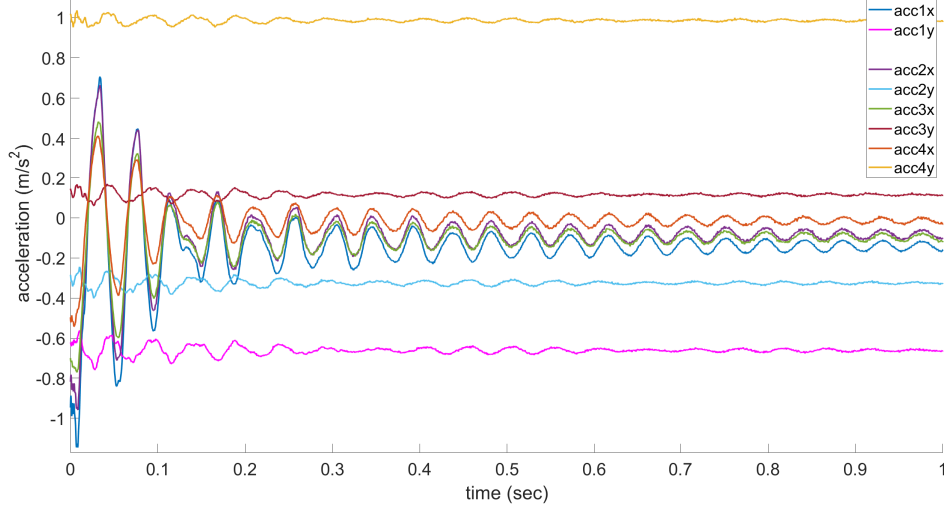
4 Monitoring of rocking modes under scour

In this Section, the natural frequencies and the center of rotation mode are identified during experiments, and scour sensitivity analysis is made by varying D . Indeed this part aims to fit a modeling with the experiments by using the results of both Section 2 and Section 3. Discussions is given at the end.

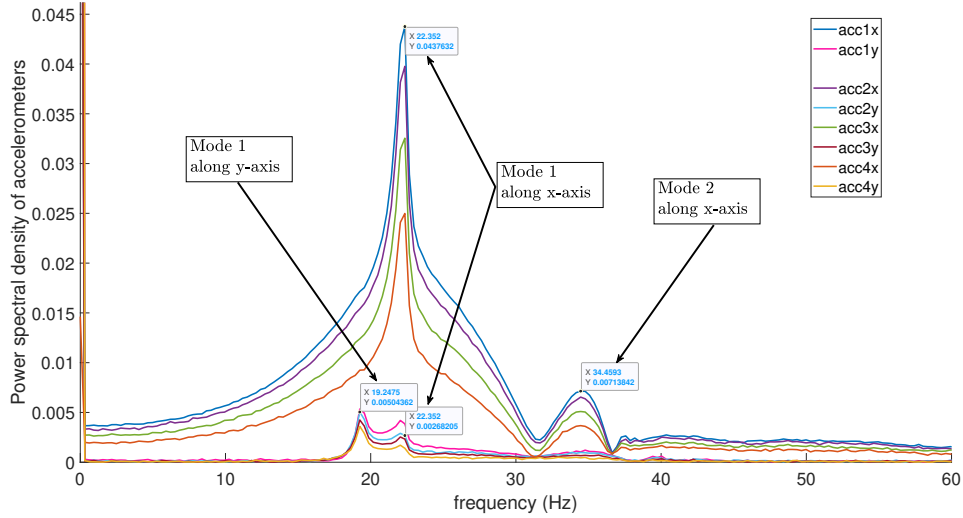
4.1 Modal parameters identification

For each reduced bridge pier presented in Table 1, the ground level is changed after each impact test. In Figure 10 via frequency domain decomposition, the identification of the two rocking modes for pier 2 is given with the same representation of Figure 9.

In Table 2, the natural frequencies (f_1, f_2) and the centers of rotation of the modes (z_{c1}, z_{c2}) are identified for all tested piers. Some test contain only one frequency because extraction of natural frequencies with peak picking method becomes difficult because of some environmental noise during experiments. Identification of center of rotation of modes identification are more difficult due to complex mode shapes. Moreover phase between sensors gives an inefficient linear regression and hypothesis according to rocking behavior assumption.



(a) Temporal response at each position for the pier 2 for $D = 30\text{cm}$



(b) Power spectral density at each position for the pier 2 for $D = 30\text{cm}$ using FFT algorithm

Figure 7: Temporal and frequency response of pier 2 for $D = 30\text{ cm}$

4.2 Discussions about model updating of the second mode

In order to update the physical model, we assume that the mass density of the concrete pier is $\rho_b = 2400\text{ kg.m}^{-3}$. Mechanical coefficient of soil are obtained from a mini-pressuremeter test [45] in order to determine the average Ménard modulus E_m [46]. The relation between Ménard modulus and young modulus of soil is described in equation 21 with $\alpha = 0.3$ for sand.

$$E_s = \frac{E_m}{\alpha} \quad (21)$$

where $E_m = 0.83\text{ MPa}$ in our case. The Young modulus of the soil and its Poisson ratio are respectively $E_s = 2.5\text{ MPa}$ and $\nu_s = 0.2$. As shown in Figure 11 the analytical second mode does not fit with experiments from EMA. We observe that the first mode corresponds to the expectations of the models. Nevertheless, for the second mode the expected results are not in accordance with the observed reality. Indeed, the eigenfrequencies of the second modes observed experimentally are lower than those expected by the rigid stack model with two degrees of freedom. And the rotation center is under estimated for this same mode. As said in Section 3, the mode is highly damped and take in account the inertia of the soil. This effects can be the cause of the unfitting curves because it may reduce the frequency by an effect of mass added (Figure 11a) and increase the position of the rotation center by a sliding effect of soil (Figure 11b).

Because of the high position of the rotation center, the second mode is very affected by soil vibrations. In this

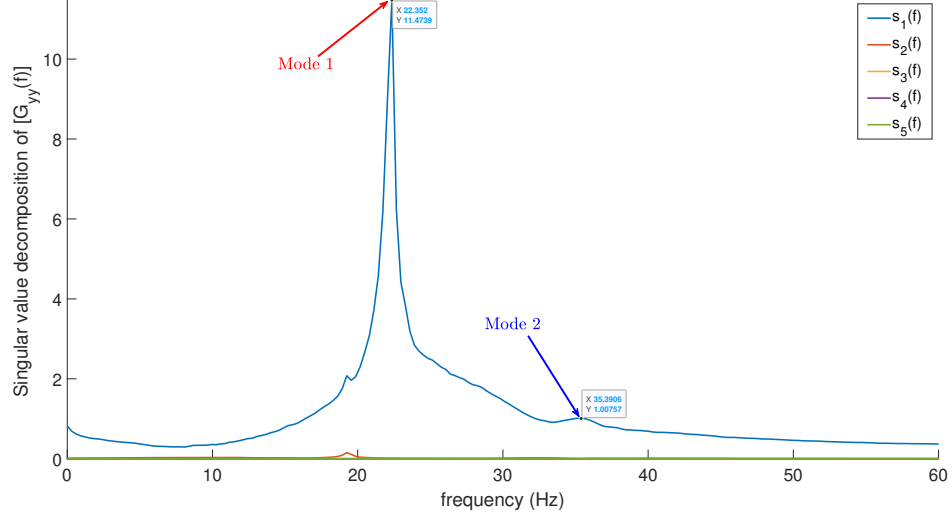


Figure 8: Frequency Domain Decomposition of pier 2 for $D=30\text{cm}$



Figure 9: Rocking shape modes of the pier 2 with $D = 30\text{cm}$.

respect Figure 12 represents a finite element model (FEM) simulation for the pier 2 with $D = 30\text{ cm}$ and with the same numerical values for E_s , ρ_b and ν_s . In Figure 12, we suppose the soil as a linear elastic material with a smooth interface between soil and structure. We also blocked displacement at the edge of the soil.

Mode 2 is still not fitting but we can observe that this second mode is a global mode considering soil inertia effect. In fact, the study considers the action from the soil as boundary reaction. However, the second mode appears as a global mode which concern soil and structure. Futures studies must at least consider the inertial of the soil as we can see in FEM simulations in Figure 12. Also, it should be complementary to the study to see the propagation of the impact test through the structure and the soil. Some information from the soil may be relevant for the second mode understanding. Moreover, as the second mode is undamped, future works should focus on damped system by considering viscous-elastic soil as Gazetas [41] proposed with a Winkler dynamic soil modelled with springs and dashpots. Also, here the soil modulus is very low. If we consider the sencond mode as a mode where the translation is important, this mode may disappear in real soil where the the rigidity is higher? New work should focus on physical modelling of soil by changing materials propriety or do experiments in a centrifuge.

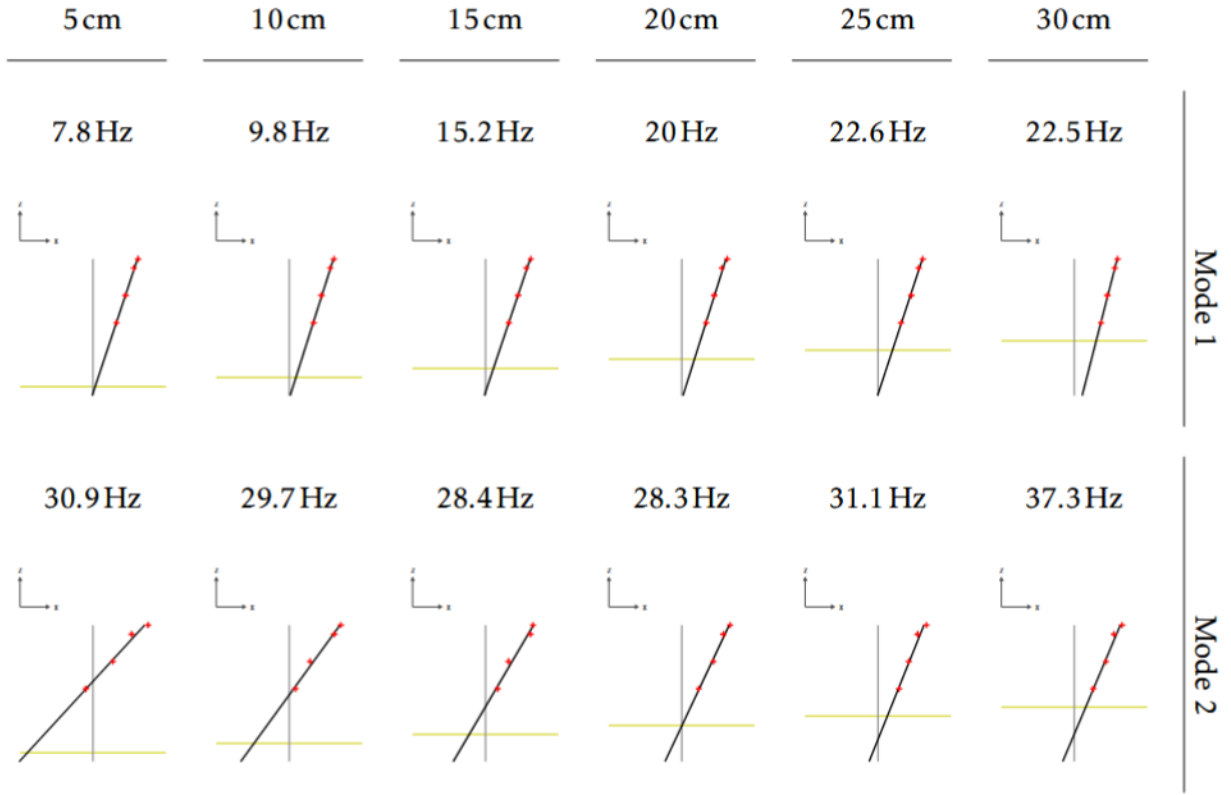


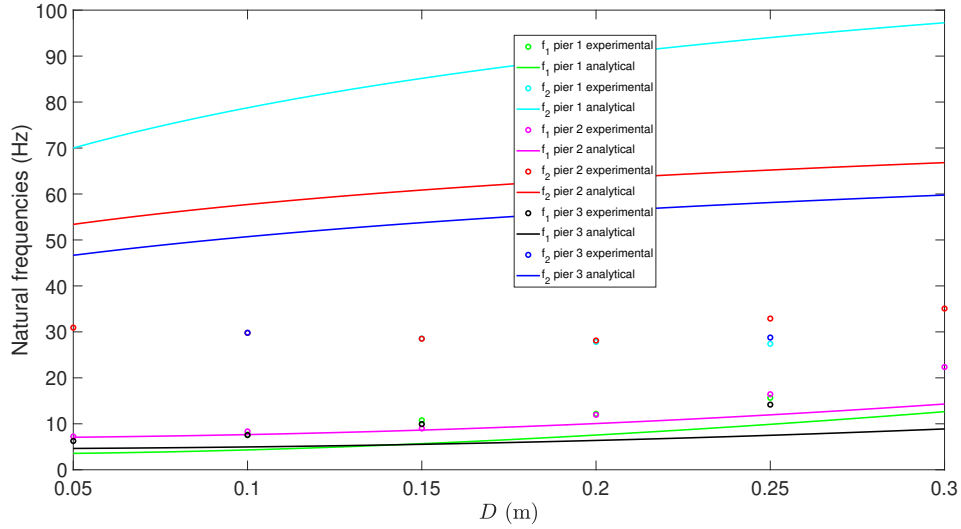
Figure 10: Experimental modal analysis for pier 2 from $D = 5\text{cm}$ to $D = 30\text{cm}$.

Table 2: Natural frequencies (f_1, f_2) and center of rotation of the modes (z_{c1}, z_{c2}) identified

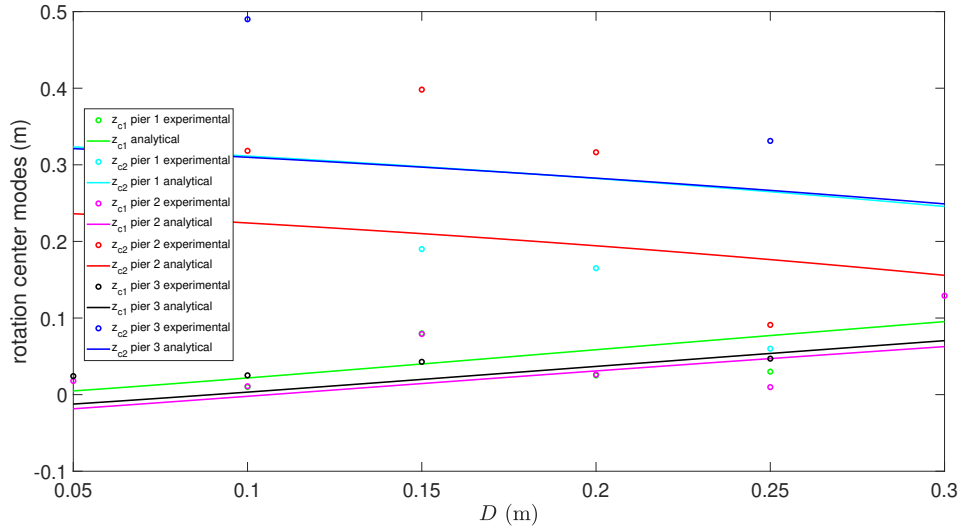
Pier n°	D (m)	f_1 (Hz)	f_2 (Hz)	z_{c1} (m)	z_{c2} (m)
1	0.1	8.9	—	0.01	—
	0.15	11.9	28.3	0.08	0.19
	0.2	15.2	28.0	0.02	0.165
	0.25	17.6	27.7	0.03	0.06
2	0.05	7.8	30.9	0.017	—
	0.1	9.8	29.7	0.011	0.32
	0.15	15.2	28.4	0.05	0.39
	0.2	20	28.3	0.02	0.31
	0.25	22.6	31.1	0.01	0.1
	0.30	22.5	37.3	—	—
3	0.05	6.4	33.7	0.02	—
	0.1	7.7	33.1	0.03	0.49
	0.15	9.9	31.5	0.04	—
	0.2	—	—	—	—
	0.25	16.3	29.0	0.05	0.13

5 Conclusion

In this paper, the rocking behavior of a bridge pier was investigated in order to study the impact of scour. Scour is here treated as a variation of the ground level of the soil which is modeled by Winkler springs in Section 2.2. Analytical and numerical simulations show the possibility to monitor scour through rocking vibration of the pier in section 2.3. This work allowed to establish the typical vibratory behavior of a bridge pier. This one is announced in Section 3.1 as a rocking model with two degrees of freedom where a rotation and a translation are allowed. From this model, it derives two modes, the first mode is a mode where the shape correspond on a rotation mode and the second one is more sensitive



(a) Natural frequencies of tested piers.



(b) Center of rotation of the modes of tested piers

Figure 11: Analytical vs EMA for the tested piers.

to translation. From Section 2.3 and Section 3.1, an experimental protocol has been set up for the identification of these mode during the Section 3. Modal parameters were presented, and a new parameter was introduced: the rotation center mode. Because of an easier interpretation and identification, this parameter is supposed to replace shape modes for modal identification and testing. Associated with natural frequencies a new method of experimental modal analysis has been proposed for the monitoring of scour phenomenon. The use of several sensors allows, on the one hand, to verify the rocking behavior of the structure. On the other hand, it allows the identification of the modes thanks to the frequency domain decomposition. The consideration of a rocking vibration mode where translations are possible at the pile anchor is an innovative aspect of this paper. However, the Section 4 highlighted limitation of the model by comparing models with experiments. In fact, in Section 4.1, the variation of modal parameter with scour (variable D) does not match for the second mode. In fact, following the choice of the initial modeling which consists in considering the effect of the ground as an elastic reaction the effect of the soil as an elastic reaction is discussed in Section 4.2. Finite element simulations show that the soil is also moving after the free response of the bridge pier. This observation lead us to propose new angles of approach by considering new soil models in Section 4.2. In short, this work allows a better understanding of dynamical response of scoured bridge pier with limits and perspectives of future works.

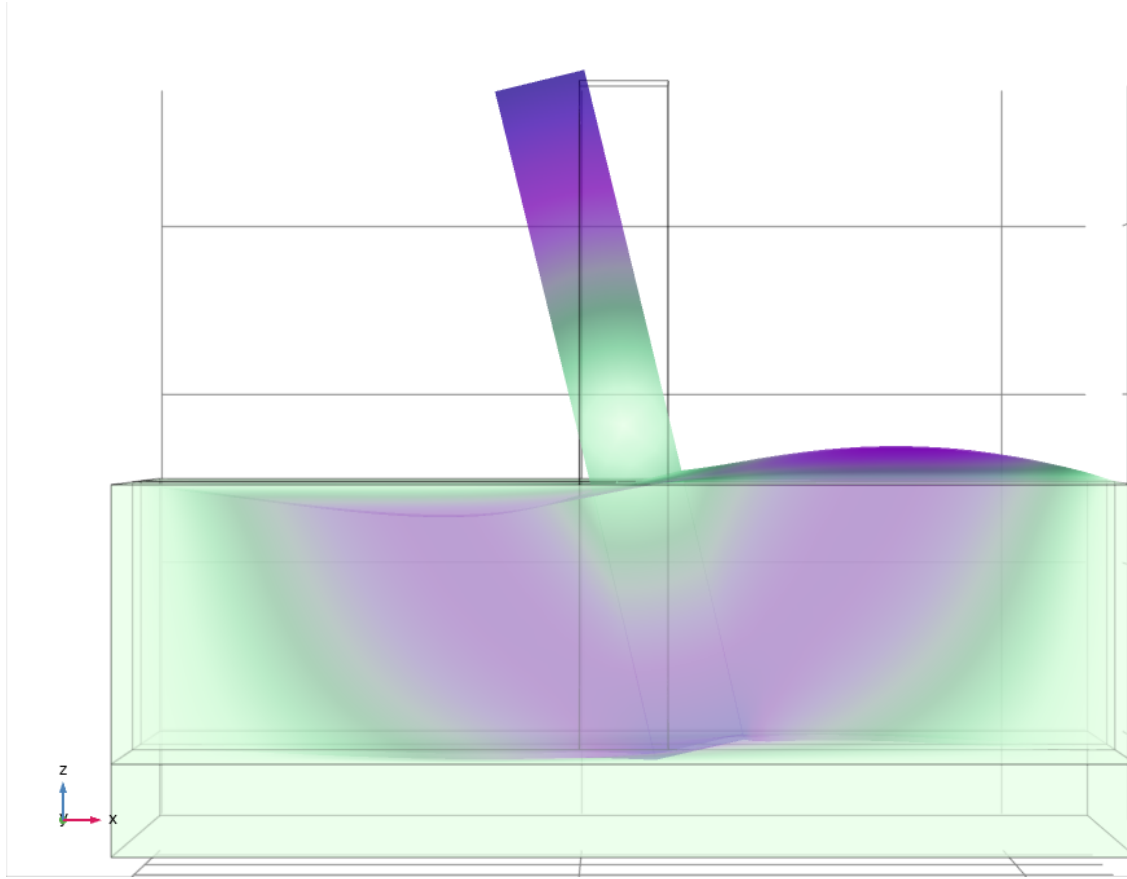


Figure 12: FEM model of mode 2 for the pier 2 with $D = 30\text{ cm}$.

Declarations

The authors declare that there are no conflict of interest or competing interest concerning the content of this paper.

References

- [1] K. Worden, C. R. Farrar, G. Manson, and G. Park, "The fundamental axioms of structural health monitoring," *Proceedings of the Royal Society A: Mathematical, Physical and Engineering Sciences*, vol. 463, no. 2082, pp. 1639–1664, 2007.
- [2] O. Avci, O. Abdeljaber, S. Kiranyaz, M. Hussein, M. Gabbouj, and D. J. Inman, "A review of vibration-based damage detection in civil structures: From traditional methods to machine learning and deep learning applications," *Mechanical Systems and Signal Processing*, vol. 147, p. 107077, 2021.
- [3] G. Kerschen, K. Worden, A. F. Vakakis, and J.-C. Golinval, "Past, present and future of nonlinear system identification in structural dynamics," *Mechanical Systems and Signal Processing*, vol. 20, no. 3, pp. 505–592, 2006.
- [4] J.-J. Sinou, "A review of damage detection and health monitoring of mechanical systems from changes in the measurement of linear and non-linear vibrations," in *Mechanical Vibrations: Measurement, Effects and Control* (R. C. Sapri, ed.), pp. 643–702, Nova Science Publishers, Inc., 2009.
- [5] R. Lin, J. Mottershead, and T. Ng, "A state-of-the-art review on theory and engineering applications of eigenvalue and eigenvector derivatives," *Mechanical Systems and Signal Processing*, vol. 138, p. 106536, 2020.
- [6] A. Kamariotis, E. Chatzi, and D. Straub, "A framework for quantifying the value of vibration-based structural health monitoring," *Mechanical Systems and Signal Processing*, vol. 184, p. 109708, 2023.
- [7] A. Vary, *The Acousto-Ultrasonic Approach*, pp. 1–21. Boston, MA: Springer US, 1988.
- [8] S. Cantero-Chinchilla, G. Aranguren, J. M. Royo, M. Chiachío, J. Etxaniz, and A. Calvo-Echenique, "Structural health monitoring using ultrasonic guided-waves and the degree of health index," *Sensors*, vol. 21, no. 3, 2021.
- [9] M. B. W. and S. E. Coleman, *Bridge scour*. Littleton, Colorado: Water Resources Publications, 1988.

- [10] E. Tubaldi, C. Antonopoulos, S. A. Mitoulis, S. Argyroudis, F. Gara, L. Ragni, S. Carbonari, F. Dezi, A. Vratsikidis, D. Pitilakis, and A. Anastasiadis, "Field tests and numerical analysis of the effects of scour on a full-scale soil–foundation–structural system," *Journal of Civil Structural Health Monitoring*, 2022.
- [11] K. Wardhana and F. C. Hadipriono, "Analysis of recent bridge failures in the united states," *Journal of Performance of Constructed Facilities*, vol. 17, no. 3, pp. 144–150, 2003.
- [12] F. Larrarte, C. Chevalier, L. Battist, and H. Chollet, "Hydraulics and bridges: A French case study of monitoring of a bridge affected by scour," *Flow Measurement and Instrumentation*, vol. 74, p. 101783, 2020.
- [13] M. Heidarpour, H. Afzalimehr, and E. Izadinia, "Reduction of local scour around bridge pier groups using collars," *International Journal of Sediment Research*, vol. 25, no. 4, pp. 411 – 422, 2010.
- [14] J.-L. Briaud, C. K. Francis Ting, H. C. Chen, G. Rao, S. P., and G. W., "SRICOS: Prediction of scour rate in cohesive soils at bridge piers," *Journal of Geotechnical and Geoenvironmental Engineering*, vol. 125, no. 4, pp. 237–246, 1999.
- [15] M. C. Forde, D. M. McCann, M. R. Clark, K. J. Broughton, P. J. Fenning, and A. Brown, "Radar measurement of bridge scour," *NDT & E International*, vol. 32, pp. 481–492, Dec. 1999.
- [16] N. E. Yankielun and L. Zabilansky, "Laboratory investigation of time-domain reflectometry system for monitoring bridge scour," *Journal of Hydraulic Engineering*, vol. 125, pp. 1279–1284, Dec. 1999.
- [17] L. Prendergast, D. Hester, K. Gavin, and J. O'Sullivan, "An investigation of the changes in the natural frequency of a pile affected by scour," *Journal of Sound and Vibration*, vol. 332, no. 25, pp. 6685–6702, 2013.
- [18] T. Lan, W. Xu, S. Zhao, F. Liu, and Y. Liu, "Advances in vibration-based scour monitoring for bridge foundations," *IOP Conference Series: Materials Science and Engineering*, vol. 1203, p. 022127, nov 2021.
- [19] M. Belmokhtar, F. Schmidt, C. Chevalier, and A. Ture Savadkoohi, "Vibration-based method for structural health monitoring of a bridge pier subjected to environmental loads," in *Experimental Vibration Analysis for Civil Engineering Structures* (Z. Wu, T. Nagayama, J. Dang, and R. Astroza, eds.), (Cham), pp. 73–82, Springer International Publishing, 2023.
- [20] M. Kato and S. Shimada, "Vibration of PC bridge during failure process," *Journal of Structural Engineering*, vol. 112, no. 7, pp. 1692–1703, 1986.
- [21] C. R. Farrar and K. Worden, "An introduction to structural health monitoring," *Philosophical Transactions of the Royal Society A: Mathematical, Physical and Engineering Sciences*, vol. 365, no. 1851, pp. 303–315, 2007.
- [22] M. J. Whelan, M. V. Gangone, K. D. Janoyan, and R. Jha, "Real-time wireless vibration monitoring for operational modal analysis of an integral abutment highway bridge," *Engineering Structures*, vol. 31, no. 10, pp. 2224 – 2235, 2009.
- [23] P. Cawley and R. D. Adams, "The location of defects in structures from measurements of natural frequencies," *The Journal of Strain Analysis for Engineering Design*, vol. 14, no. 2, pp. 49–57, 1979.
- [24] N. M. M. Maia and J. M. M. Silva, "Modal analysis identification techniques," *Philosophical Transactions: Mathematical, Physical and Engineering Sciences*, vol. 359, no. 1778, pp. 29–40, 2001.
- [25] J. B. Bodeux and J. C. Golival, "Application of ARMAV models to the identification and damage detection of mechanical and civil engineering structures," *Smart Materials and Structures*, vol. 10, pp. 479–489, jun 2001.
- [26] S. Foti and D. Sabia, "Influence of foundation scour on the dynamic response of an existing bridge.," *Journal of Bridge Engineering*, vol. 16, no. 2, p. 295–304, 2011.
- [27] T. Iwinski, "Chapter 2: Theory of beams," pp. 14 – 70, Pergamon, second edition ed., 1967.
- [28] R. W. Yeung, "Added mass and damping of a vertical cylinder in finite-depth waters," *Applied Ocean Research*, vol. 3, pp. 119–133, July 1981.
- [29] L. J. Prendergast, D. Hester, K. Gavin, and J. J. O'Sullivan, "An investigation of the changes in the natural frequency of a pile affected by scour," *Journal of Sound and Vibration*, vol. 332, pp. 6685–6702, Dec. 2013.
- [30] N. Boujia, F. Schmidt, C. Chevalier, D. S., and D. Pham van Bang, "Effect of Scour on the Natural Frequency Responses of Bridge Piers: Development of a Scour Depth Sensor," *Infrastructures*, vol. 4, p. 21, June 2019.
- [31] N. Boujia, F. Schmidt, C. Chevalier, D. Siegert, and D. Pham Van Bang, "Using rocking frequencies of bridge piers for scour monitoring," *Structural engineering international*, p. 20 p., Jan. 2020.
- [32] M. Belmokhtar, F. Schmidt, A. Ture Savadkoohi, and C. Chevalier, "Scour monitoring of a bridge pier through eigenfrequencies analysis," *SN Applied Sciences*, vol. 3, p. 303, Feb. 2021.
- [33] S. P. Heylen W., Lammens S., *Modal Analysis, Theory and testing*. KU Leuven, Belgium, 2013.
- [34] T. Bao, R. A. Swartz, S. Vitton, Y. Sun, C. Zhang, and Z. Liu, "Critical insights for advanced bridge scour detection using the natural frequency," *Journal of Sound and Vibration*, vol. 386, pp. 116 – 133, 2017.

- [35] T. Bao, Z. Liu, and K. Bird, “Influence of soil characteristics on natural frequency-based bridge scour detection,” *Journal of Sound and Vibration*, vol. 446, pp. 195–210, Apr. 2019.
- [36] N. Boujia, F. Schmidt, C. Chevalier, D. Siegert, and D. P. V. Bang, “Using rocking frequencies of bridge piers for scour monitoring,” *Structural Engineering International*, vol. 31, no. 2, pp. 286–294, 2021.
- [37] E. Winkler, “Die Lehre von der Elastizität und Festigkeit (on elasticity and fixity) dominicus,” 1867.
- [38] G. Gazetas, “Analysis of machine foundation vibrations: State of the art,” *International Journal of Soil Dynamics and Earthquake Engineering*, vol. 2, no. 1, pp. 2–42.
- [39] G. Gazetas, “Formulas and charts for impedances of surface and embedded foundations,” *Journal of Geotechnical Engineering*, vol. 117, no. 9, pp. 1363–1381, 1991.
- [40] N. T. Novak M and Aboul-Ella, “Dynamic soil reactions for plane strain case,” *J Eng Mech*, vol. 104, no. 4, pp. 953–959, 1978.
- [41] N. Makris and G. Gazetas, “Displacement phase differences in a harmonically oscillating pile,” *Géotechnique*, vol. 43, no. 1, pp. 135–150, 1993.
- [42] Varun, D. Assimaki, and G. Gazetas, “A simplified model for lateral response of large diameter caisson foundations—linear elastic formulation,” *Soil Dynamics and Earthquake Engineering*, vol. 29, no. 2, pp. 268–291, 2009.
- [43] G. Gazetas, I. Anastasopoulos, O. Adamidis, and T. Kontoroupi, “Nonlinear rocking stiffness of foundations,” *Soil Dynamics and Earthquake Engineering*, vol. 47, pp. 83–91.
- [44] R. Brincker, L. Zhang, and P. Andersen, “Modal identification of output-only systems using frequency domain decomposition,” *Smart Materials and Structures*, vol. 10, pp. 441–445, jun 2001.
- [45] F. Baguelin, “The pressuremeter and foundation engineering,” *Trans. Tech. Publications*, 1978.
- [46] K. Terzaghi, R. B. Peck, and G. Mesri, *Soil mechanics in engineering practice*. John wiley & sons, 1996.